Available online at www.sciencedirect.com
ScienceDirect
Ceramics International 34 (2008) 1753–1762
CERAMICS INTERNATIONAL
www.elsevier.com/locate/ceramint

Wetting and penetration of cordierite and mullite materials by non-stoichiometric cordierite liquids

M.A. Camerucci *, A.L. Cavalieri

Instituto de Investigaciones en Ciencia y Tecnología de Materiales (INTEMA), Universidad Nacional de Mar del Plata-CONICET, Juan B. Justo 4302 (7600) Mar del Plata, Argentina

Received 12 March 2007; received in revised form 26 March 2007; accepted 14 June 2007
Available online 17 August 2007

Abstract

The wetting and penetration of two non-stoichiometric cordierite liquids (labelled G1 = 25 wt.% Al_2O_3, 63 wt.% SiO_2 and 12 wt.% MgO, and G2 = 20 wt.% Al_2O_3, 64 wt.% SiO_2 and 16 wt.% MgO) on sintered cordierite and mullite substrates were investigated. Their chemical compositions (G1 and G2) correspond to those glasses present in materials sintered from a commercial powder of non-stoichiometric cordierite powder at 1450 or 1400 °C, respectively.

Sessile drop assemblies for wetting and penetration tests, consisting of cordierite or mullite disks as substrates and pellets of pressed powder glasses positioned above them, were employed. Commercially available cordierite and mullite powders were used to prepare the substrates by uniaxial pressing and sintering at 1450 and 1700 °C, 2 h, respectively. The glass pellets were prepared by uniaxial pressing of G1 and G2 glass powders. The assemblies were heating at 25 °C/min up to 1450 or 1400 °C depending on each glass, soaking at these temperatures for 10, 120 or 360 min and cooling at 25 and 5 °C/min down to 1100 °C and room temperature, respectively. The contact angles between each glass and both cordierite and mullite substrates according to the temperature, were determined by heating microscopy technique from optical images. Their penetration behavior of both glasses into cordierite or mullite substrates were also studied analyzing by SEM the microstructures of the specimens transversally cut, polished, and chemically etched.

Keywords: D. Cordierite; D. Mullite; Non-stoichiometric Cordierite Glass; Wetting; Penetration

1. Introduction

Cordierite ($2Al_2O_3{\cdot}5SiO_2{\cdot}2MgO$) and cordierite–mullite ($3Al_2O_3{\cdot}2SiO_2$) ceramics are promising materials for electronic applications, among others, because of their low dielectric constant, high resistivity, elevated thermal and chemical stability, and very low thermal expansion coefficient [1–3].

Based cordierite ceramics present a very narrow sintering temperature range and are easily sintered with sintering aids in order to operate a liquid-phase process close to their melting point (1460 °C). Unfortunately, the use of sintering aids may produce deleterious effects on the thermal and electrical properties. In addition, the cordierite–mullite composites sinter much more rapidly once the cordierite has melted. However, unless substantial liquid is present, the relatively high wetting angle between mullite and cordierite liquid limits the penetration of mullite–mullite contacts [4,5].

The importance of cordierite and mullite wetting by a glass phase, especially in the early stages of liquid-phase sintering, has been thoroughly discussed in the literature [5–9]. During the firing process, the glass phase becomes more fluid when increasing temperature, migrating either to the ceramic or the porous depending on their physical structure and the wetting behavior of the liquid phase. The contact angle, the flow of glass through the network of particle interstices, and pore-filling capability of liquid are parameters that describe the grain rearrangement process. Other properties of the liquid phase, such as viscosity, solubility, and diffusion of the solid in the liquid are very important and must be considered when a liquid-phase sintering mechanism is operating.

The aim of this paper is to study both, the wetting behavior of two non-stoichiometric cordierite liquids on cordierite and

* Corresponding author. Tel.: +54 223 4816600; fax: +54 223 4810046.
E-mail address: andcamer@fi.mdp.edu.ar (M.A. Camerucci).

0272-8842/$34.00
doi:10.1016/j.ceramint.2007.06.013

mullite substrates and their penetration degrees into these dense ceramic materials in order to clarify the influence of these liquids in the sintering mechanism of cordierite–mullite composites.

2. Experimental

2.1. Materials and techniques

Two non-stoichiometric cordierite glasses labelled as G1 and G2 were prepared. Their chemical compositions were 25 wt.% Al_2O_3, 63 wt.% SiO_2 and 12 wt.% MgO (G1) and 20 wt.% Al_2O_3, 64 wt.% SiO_2 and 16 wt.% MgO (G2). These compositions correspond to the glasses present together with cordierite and mullite crystalline phases in the materials sintered at 1450 or 1400 °C, respectively from a commercial non-stoichiometric cordierite powder [8,9].

The glasses were prepared from submicronic powders of α-corundum, α-quartz and MgO. The oxide mixtures were melted in a platinum crucible at 1600 °C for 2 h in an electric furnace and quenched in water at room temperature. The fragmented glasses were dried in a stove and then milled in agate mortar to obtain a granulometric fraction (50 wt.% < 37 μm). Their picnometric densities (δ_{pic}) were determined in kerosene at 37 °C. The qualitative X-ray diffraction analysis (XRD) was done at 30 mA and 40 kV using Cu Kα radiation, Ni filter and a scan rate of 1° min^{-1} in the $\theta/2\theta$ measurement (Philips X-ray diffractometer). Glass viscosities, η were evaluated by heating microscopy as a function of the temperature (Leitz microscope). The Vogel–Fulcher–Tamman equations $\log \eta = 1.827273 + 121.4876/(T - 1354.545)$, $r^2 = 1$ (T = temperature, 1380–1450 °C) and $\log \eta = 2.039 + 104.982/(T - 1302.365)$, $r^2 = 0.91$ (T = temperature, 1320–1410 °C) were used by fitting the experimental data.

The differential thermal analyses (DTA) were performed in air at 5 °C/min (Shimadzu DTA-50) up to 1300 °C.

In order to estimate the surface tension for the liquid–vapor interfaces, γ_{LV} for both G1 and G2 liquids, a relation that considers their chemical compositions was employed, $\gamma = \sum_i(\gamma_i m_i)/100$, where γ_i is the tension coefficient corresponding to each oxide i (tabulated values) and m_i is its molar percentage [10].

Commercially available high purity powders of cordierite (CORCR Baikowski, France) and mullite (MUL Baikowski, France) were used to prepare the substrates. Their mean particle sizes were $D_{50} = 1.82$ μm and $D_{50} = 2.10$ μm, respectively (Coulter LS 130 analyzer) and their specific surface areas BET were $S_S = 3.4$ m^2/g and $S_S = 2.3$ m^2/g, respectively (Monosorb Quantachrome equipment). XRD powder patterns of as-received powders were recorded at 30 mA and 40 kV using Cu K_α radiation, a Ni filter and a scan rate of 1° min^{-1} in the $\theta/2\theta$ measurement (Philips X-ray diffractometer).

Cordierite and mullite disks with a thickness/diameter ratio equal 0.25 (1.2 cm in diameter × 0.3 cm in height) were formed by uniaxial pressing at 18 MPa without binders employing a lubricated steel cylindrical mold. These cordierite and mullite green disks were sintered at 1450 °C and 1700 °C for 2 h, respectively [8,9] in an electrical furnace with $MoSi_2$ heating elements. A slow heating schedule was employed: heating at 25 °C/min up to 800 °C and 5 °C/min up to each sintering temperature; cooling at 10 °C/min down to 800 °C and free cooling down to room temperature.

The apparent densities of the sintered materials (δ_S) were measured by Archimedes method in distilled water. The porosity percentages ($100 - \%\delta_S/\delta_R$) were calculated using the corresponding real densities ($\delta_{R\ cordierite} = 2.57$ g/cm^3 and $\delta_{R\ mullite} = 3.05$ g/cm^3 [8,9]) of the powders treated at the respective sintering temperature (1450 or 1700 °C, respectively).

The microstructures of the sintered substrates were analyzed by scanning electron microscopy (SEM) on polished surfaces with 6, 3 and 1 μm diamond pastes and thermally etched. Image analysis (Image-Pro Plus software) to measure grain sizes (about 200–300 grains) on the SEM photographs was used in order to determine the average grain size.

The roughness characteristics of the substrates (Ra; Rs) were measured with a Surtronic 3 + (Taylor Hobson) surface profilometer equipped with a 1 μm diamond stylus tip. A traverse length of 1.25 mm and a cut-off length of 0.25 mm were used.

2.2. Wetting and penetration assemblies

For wetting and penetration studies, sessile drop assemblies were used. They consisted of cordierite and mullite substrates with a glass cylindrical pellet (G1 or G2) positioned on them. These pellets (0.3 mm in thick and 0.5 mm in diameter) of both milled glass powders (G1 and G2) were prepared by uniaxial pressing at 10 MPa. The cordierite and mullite substrate surfaces were ultrasonically cleaned in isopropyl alcohol, prior to wetting and penetration tests.

The wetting behavior of non-stoichiometric cordierite liquids on dense sintered cordierite and mullite substrates was evaluated by measuring the contact angles between the liquids and the substrates as a function of the temperature. The wetting behavior of sessile drops was defined by the contact angle subtended at the drop periphery by the liquid surface and the liquid-solid interface. Optical images between the glassy phases and both, cordierite and mullite substrates as a consequence of the increasing temperature, were acquired by heating microscopy technique. At each temperature, contact angles were calculated from these images as the average measurements of both sides of the drop. These measurements on cordierite and mullite substrates were between ±2° and ±4° for G1 and ±3° and ±4° for G2, respectively.

Moreover, from the sessile drop tests, the melting and the fluidity points of G1 and G2 liquids were also determined. The melting point (T_m) was considered as the base equal to two heights and the fluidity point (T_f) as the base equal to seven heights.

For penetration tests, the assembles were covered with an inverted platinum crucible and placed in an electrical furnace with $MoSi_2$ elements. A liquid glass drop was formed during

the heating. The assembly was heated at 25 °C/min up to 1450 or 1400 °C depending on each glass (G1 or G2, respectively) and soaking at these temperatures for 10, 120 or 360 min. After that, the temperature was lowered with the following heating schedule: at 25 °C/min to 1100 °C (temperature always higher than Tg_{G1} and Tg_{G2}) and at 5 °C/min to room temperature. This process annealed the glass drop formed during heating.

After penetration tests, samples were analyzed by scanning electron microscopy (SEM) in order to evaluate the penetration of both liquids into both substrates. They were perpendicularly sectioned to the interface with a diamond wafering saw and they inlaid into polyester resin. The grinding and polishing of these samples was sequentially carried out using SiC papers (320 and 600 grit) and diamond pastes (6, 3 and 1 μm), followed by a chemical etching (15 s in 10% HF).

3. Results and discussion

3.1. Characterization of the non-stoichiometric cordierite glasses

The studied glasses (G1 and G2) were located in the cordierite crystallization field in the isothermal sections of the Al_2O_3–SiO_2–MgO system at 1450 and 1400 °C, respectively [11].

Their picnometric densities (δ_{pic}) were 2.51 g/cm^3 for G1 and 2.47 g/cm^3 for G2. These values were low in respect to stoichiometric cordierite glass density (2.63–2.64 g/cm^3) [12]. This can be explained considering that both glasses possess different chemical compositions with regard to stoichiometric cordierite glass composition (34.8 wt.% Al_2O_3; 51.4 wt.% SiO_2 and 13.8 wt%. MgO). G1 and G2, have higher amounts of SiO_2 (network forming) and lower amounts of Al_2O_3 (network conditional forming). In addition, G2 has a higher amount of MgO (network modifying).

In XRD patterns of both G1 and G2 glasses (Fig. 1a and b), a wide band of very low intensity appears between 10 and 30° 2θ, zone of the main diffraction peaks of μ- and α-cordierite crystalline phases (JCPDS Powder Diffraction Data Cards N° 14-249 and 13-293, respectively).

Viscosities of both glasses strongly decrease by increasing the temperature (Fig. 2) as expected for glasses with a great tendency to devitrify and high glass transition temperatures (Tg_{G1} = 830 °C; Tg_{G2} = 840 °C). Despite this, both glasses shown similar viscosities at higher temperatures (1450 and 1400 °C, respectively), the viscosity for G1 decreased more quickly by increasing the temperature. This fact could be associated with its greater tendency to crystallize.

For G1 and G2 liquids, as was expected, the values of the melting (T_m) and the fluidity (T_f) points kept independent of the substrate material. For G1, T_m and T_f were about 1390 °C and 1420 °C, respectively, and for G2, T_m and T_f were 1340 °C and 1360–1380 °C, respectively.

In DTA curves for both glasses, one endothermic peak and three exothermic peaks were registered (Fig. 3). Taking into account the obtained XRD results (Fig. 1a and b) [13], the first peak was assigned to nucleation and/or sintering and the others

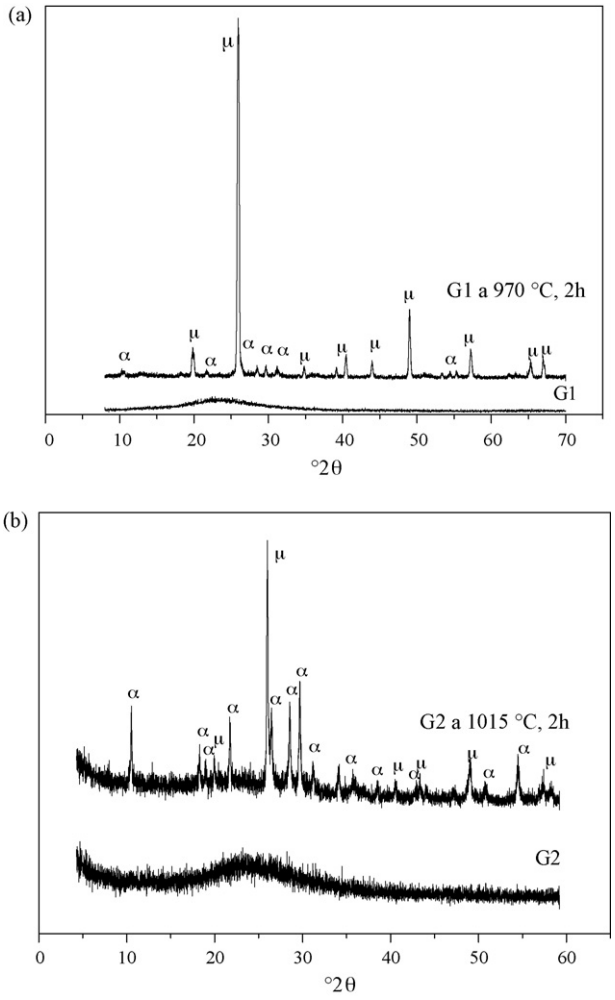

Fig. 1. XRD patterns of: (a) G1 and G1 treated at 970 °C for 2 h and (b) G2 and G2 treated at 1015 °C for 2 h.

were attributed to crystallization of μ-cordierite (970 °C for G1 and 1015 °C for G2) and α-cordierite (1060 and 1170 °C for G1 and 1165 and 1268 °C for G2). The lower crystallization temperatures were registered in G1 glass in agreement with its greater tendency to crystallize. Moreover, for both glasses these temperatures were higher than those of stoichiometric cordierite glass [14–16]. The higher stability of the μ-phase

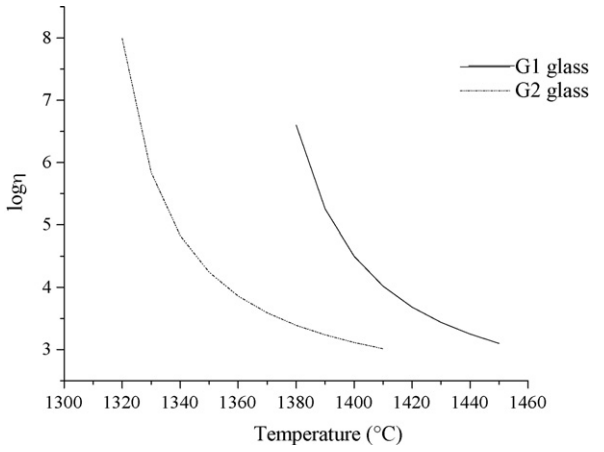

Fig. 2. Viscosity of G1 and G2 glasses as a function of the temperature.

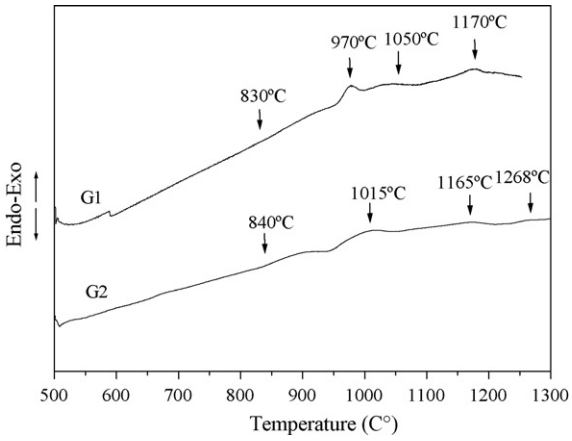

Fig. 3. DTA curves for G1 and G2 glasses.

that occurs with excess of SiO_2 or lower amounts of Al_2O_3 or MgO in the composition, as occurred in both studied glasses, can explain the delay produced in the α-cordierite crystallization with regard to the stoichiometric glass [16].

The estimated interfacial tensions for the liquid–vapor interfaces, γ_{LV} were similar for both, G1 and G2 liquids: 382 and 383 dyn/cm, respectively.

3.2. Characterization of cordierite and mullite substrates

In the Al_2O_3–SiO_2–MgO ternary system [11], the composition of the commercial cordierite powder was located in the crystallization field of mullite shifted to the alumina corner from the cordierite stoichiometric composition (SiO_2 = 51.4%, Al_2O_3 = 34.8% and MgO = 13.8%), in the cordierite–mullite–silica compatibility triangle. The calculated weight percentages of these phases were 92% cordierite, 7% mullite and 1% silica.

Moreover, the mullite powder was located on the Al_2O_3–SiO_2 binary side shifted to the silica corner from the mullite stoichiometric composition (SiO_2 = 28.2%, Al_2O_3 = 72.8%). A composition of 91% mullite and 9% silica as cristobalite was calculated.

Two crystalline phases, α-cordierite (JCPDS Powder Diffraction Data Card N° 13-293) and mullite (JCPDS Powder Diffraction Data Card N° 15-776), were identified by XRD analysis in the commercial cordierite powder. Silica was not determined using this technique [9]. Characteristic diffraction peaks of mullite and α-cristobalite (JCPDS Powder Diffraction Data Card N° 39-425) were observed in XRD pattern of the mullite powder.

At the sintering temperature of cordierite substrate (1450 °C), the composition of the commercial cordierite powder was located in the crystallization field of mullite, in the cordierite–mullite-liquid compatibility triangle close to the cordierite stoichiometric composition (SiO_2 = 51.4%, Al_2O_3 = 34.8% and MgO = 13.8%). The present phases were cordierite, mullite and liquid of G1 composition, and the calculated weight percentages obtained were 84% cordierite, 10% mullite and 6% liquid.

According to Aramaki and Roy's equilibrium diagram [17], the commercial mullite powder (Al_2O_3 = 65.3% and SiO_2 = 25.7%) at the sintering temperature of mullite substrate (1700 °C) was composed by 87 wt.% mullite and 13 wt.% liquid (SiO_2 = 83% and Al_2O_3 = 17%).

Table 1
Apparent densities (δ_S), densification degree ($\%\delta_S/\delta_R$), and porosity ($\%P$) of cordierite and mullite sintered substrates

Substrates	Sintering temperature (°C)	δ_S (g/cm^3)	$\%\delta_S/\delta_R$	$\%P = (100 - \delta_S/\delta_{pic})$
Cordierite	1450	2.44 ± 0.01	95.15	4.95
Mullite	1700	3.07 ± 0.02	97.03	2.97

The apparent densities of the sintered substrates (δ_S), densification degree, ($\%\delta_S/\delta_R$) and porosity ($\%P$) achieved in cordierite and mullite substrates sintered at 1450 °C for 2 h and 1700 °C for 2 h, respectively, are shown in Table 1.

SEM photographs of the cordierite and mullite sintered substrates are shown in Fig. 4a and b, respectively. The cordierite microstructure resulted rather homogeneous with mainly equiaxial grains of submicronic size and spherical pores with sizes close to grain sizes. In mullite, more faceted grains and some elongated ones (aspect ratio about ≈ 1.9) were observed together with less amount of porous of higher size than the present in cordierite substrate. The average grain sizes

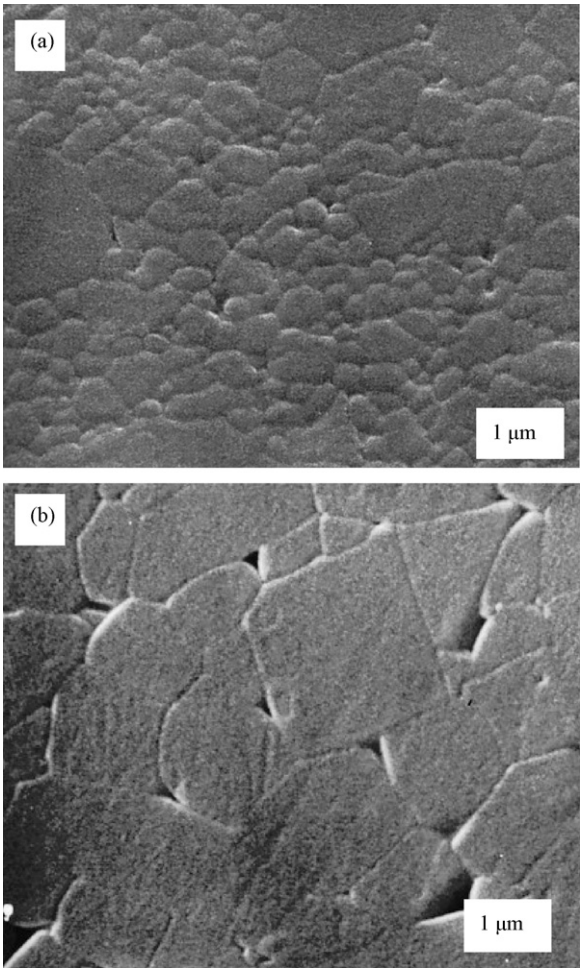

Fig. 4. SEM photographs of the (a) cordierite and (b) mullite substrates sintered. Bars = 1 μm.

Table 2
Ra and Rs average values and Ra/Rs ratio of cordierite and mullite substrates

Substrates	Ra (μm)	Rs (μm)	Ra/Rs
Cordierite	0.45 ± 0.21	13.9 ± 3.2	0.032
Mullite	0.58 ± 0.02	15.5 ± 1.1	0.037

of cordierite and mullite resulted equal to 0.46 ± 0.20 and 0.95 ± 0.59 μm, respectively, both lower than the starting particle size, indicating the occurrence of a rearrangement step in the liquid-phase sintering [8,9].

In ceramics systems at high temperature, the wetting is more complex than the suggested by the Young equation ($\gamma_{sl} + \gamma_{lv} \cos\theta = \gamma_{sv}$, where γ is the interface energy and s, l and v are solid, liquid and vapor, respectively) and variables such as surface roughness and dissolution reactions are significant. In several works, to minimize the effect of surface roughness on wetting behavior, the substrates were ground and polished down to 1 μm diamond paste [5,18–20]. In this work, the as-sintered cordierite and mullite substrates were used. However, the surface condition was evaluated from roughness measurements and it was taken into account in the wetting analysis. The values of Ra (average deviation of the surface profile with regard to the central line) and Rs (average distance between two consecutive peaks) parameters and the Ra/Rs ratio were used in order to characterize the randomly rough surfaces (Table 2). For both sintered materials, both Ra and Rs values resulted similar and consequently an insignificant difference between the Ra/Rs ratios was determined. According to these surface features, it was assumed that cordierite substrates look alike mullite ones, affecting the wetting in a similar way with regard to the polished surfaces.

3.3. Wetting behaviour

The sequential images of the wettability tests (Fig. 5A and B) represent the evolution of both liquids (G1 and G2) on both, the cordierite and the mullite substrates by increasing the temperature. It can be observed that the liquids spread uniformly on cordierite substrate as well as on mullite substrate, discarding the presence of bubbles in the liquids that would invalidate the measurements of the contact angles. Both glasses exhibited a better wettability on cordierite that on mullite in agreement with data reported for cordierite liquids on the same substrate materials [4,5].

It is noteworthy that higher Ra/Rs ratios increase the contact angles (decrease the substrate wettability) being this dependence lower at higher temperatures [20]. Taking into account this dependence, the contact angles between non-stoichiometric cordierite liquids and cordierite or mullite substrates could result overestimated due to the fact that the measurements were accomplished on as-sintered surfaces. In Fig. 6, the average contact angles as a function of temperature are given. The contact angles of G1 and G2 liquids on both cordierite and

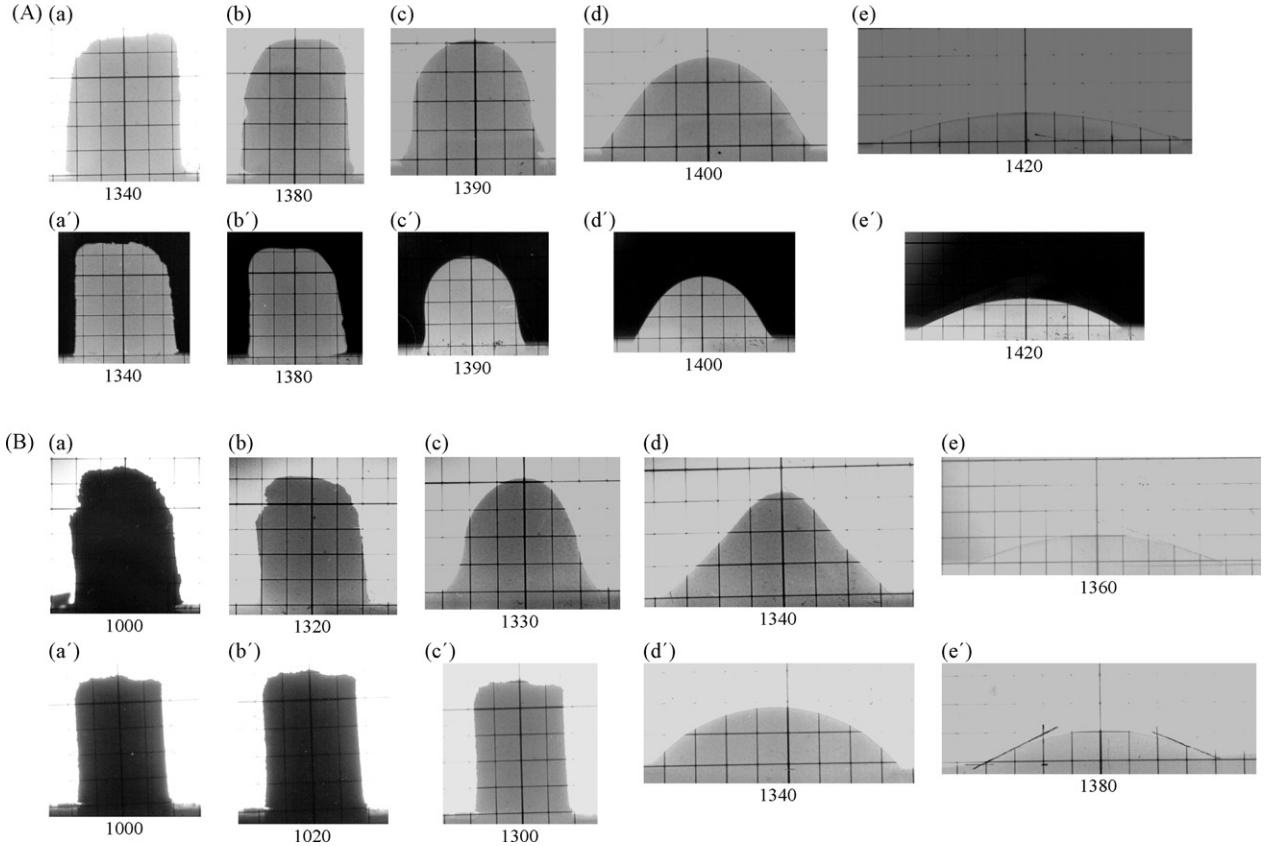

Fig. 5. Sequential images of the wettability tests by increasing temperature for (A): G1 on cordierite (a–e) and mullite (a′–e′) substrates and, (B): G2 on cordierite (a–e) and mullite (a′–e′) substrates.

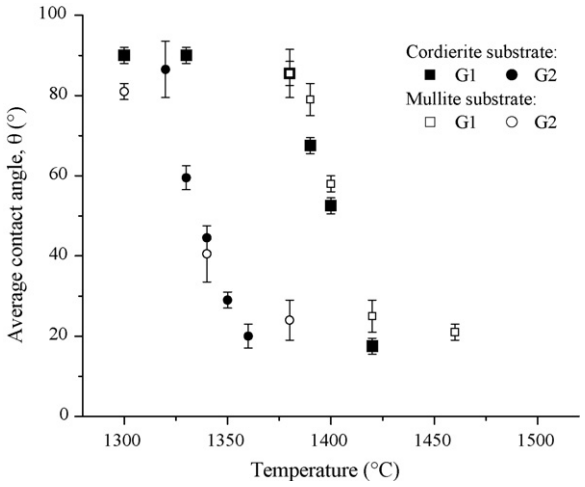

Fig. 6. Variation of average contact angles for G1 and G2 liquids with temperature.

mullite substrates decreased as the temperature increased. According to Young's equation, the γ_{LV}/γ_{SL} ratio increases when the contact angle decreases. Therefore, the solid/liquid interfacial energies decrease, resulting in greater wettability at highest temperatures. In order to avoid the difficult determinations of γ_{SL} and γ_{SV}, the Gibbs energy change can be calculated as a function of liquid–vapor interfacial energy: $\Delta G = -\gamma_{LV}(1 + \cos\theta)$ [19]. Then, the lower the values of the contact angles, the higher wetting since ΔG decreases. This relationship assumes chemical equilibrium and, therefore, that the surface of the drop remains spherical in curvature. Experimentally, this assumption is essentially fulfilled for small enough sessile drops. By assuming such condition and based on the light of the results, both liquids wet both substrates ($\theta < 90^\circ$); however, the spreading or complete wetting ($\theta = 0^\circ$) did not occur. For two substrate materials, the initial spreading temperature increased for G1 composition. For both, G1 and G2, the contact angle at highest temperature on cordierite substrate was lower than the obtained on mullite one: $\sim 20^\circ$ on cordierite substrates and slightly higher ($\sim 25^\circ$) on mullite. The obtained contact angle values were in the range of those reported in similar systems [4,5].

3.4. Penetration tests

It is noteworthy that while the sessile drop analysis is concerned with the solid–liquid and vapour-phase chemical equilibrium at the periphery, the study under nonequilibrium conditions is primarily concerned with equilibria at the solid–liquid interface. Under conditions of chemical nonequilibrium,

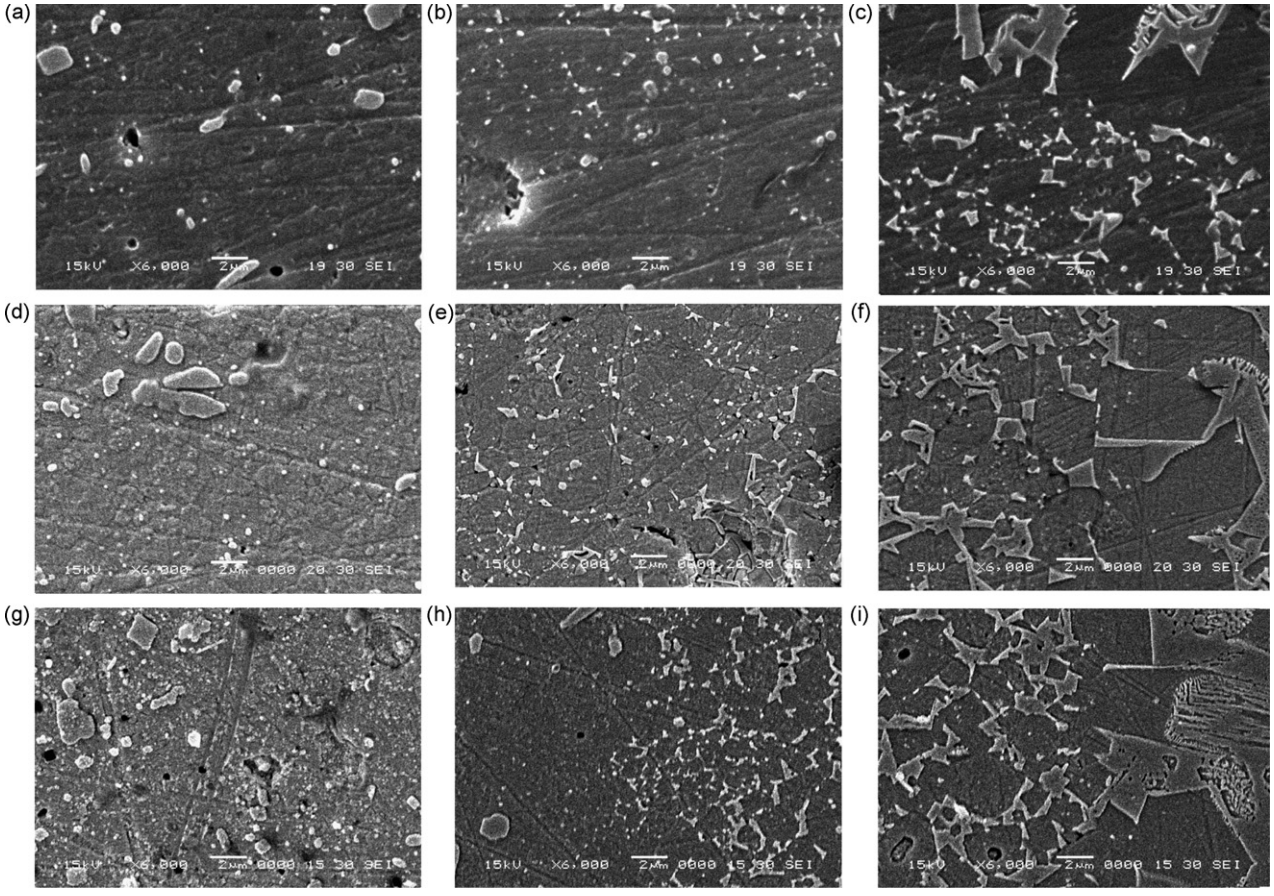

Fig. 7. SEM photomicrograph of three zones of the cordierite cross-section after 10 min ((a) distant extreme of the G1 glass/cordierite interface; (b) middle zone; (c) zone adjacent to G1 glass/cordierite interface); 120 min ((d) distant extreme of the G1 glass/cordierite interface, e: middle zone; (f) zone adjacent to G1 glass/cordierite interface) and 360 min ((g) distant extreme of the G1 glass/cordierite interface; (h) middle zone; (i) zone adjacent to G1 glass/cordierite interface). Bars = 2 μm.

reactions at the interface will proceed until the equilibrium is achieved and they will influence the transient wetting behavior. In a wetting and nonreactive system, and in absence of open porous into solid phase, a potential driving force for penetration would exist making it necessary to have a reactive none-quilibrium system along the interfaces in order to have penetration. The solution reaction provides channel for liquid movement and, therefore, it develops a driving force for penetration.

The penetration into cordierite and mullite substrates of G1 and G2 glasses was studied as a function of the dwell time (10, 120 and 360 min) at 1450 or 1400 °C, respectively. Two different types of location of the glasses, three-grain junctions and grain–grain interfaces, were distinguished when the features of penetration of G1 and G2 glasses into the substrates considering dwell time at the corresponding temperature (1450 or 1400 °C) were analyzed.

SEM photomicrographs of the developed microstructures along cross-section of G1 and G2 liquid/cordierite interfaces are shown in Figs. 7 and 8, respectively. In both figures, the increase of the glasses penetration across mainly open pores of the cordierite substrates from interphase substrate/glass (Fig. 7c, f and i) towards the distant extreme (Fig. 7a, d and g) and their crystallization by increasing time were clearly observed. The crystallization of both glasses was supported by the presence of dendrites and/or hexagonal crystals attributed a μ- and α-cordierite phases [13,21].

In the case of the G1 glass into cordierite substrate, the crystallization occurred for 10 min in agreement with its high tendency to devitrify and the high temperature of the test (1450 °C), resulting very difficult to distinguish its location: in triple points and/or grain–grain interfaces.

The penetration of G2 through the pores connected to the surface was also appreciated, while a similar crystallization to G1 glass was observed at 360 min (Fig. 8h and i). At shorter times (10 and 120 min), the glass penetrated; however, its crystallization did not occur. At these times, triple points and grain–grain boundaries were developed by chemical etching. In a zone close to the interface, the glass was observed predominantly located in grain boundaries while at areas further into cordierite microstructure it was principally appreciated in the three-grain junctions.

Based on these results, both glasses shown different behaviors considering time: the G1 glass penetrated and crystallized fast; while G2, although it also penetrated, its crystallization was only observed at longest time studied. Moreover, in the case of G2 glass and considering that the penetration test temperature (1400 °C) was close to the equilibrium temperature of the glass present into cordierite substrates, a reaction at the solid–liquid interfaces until

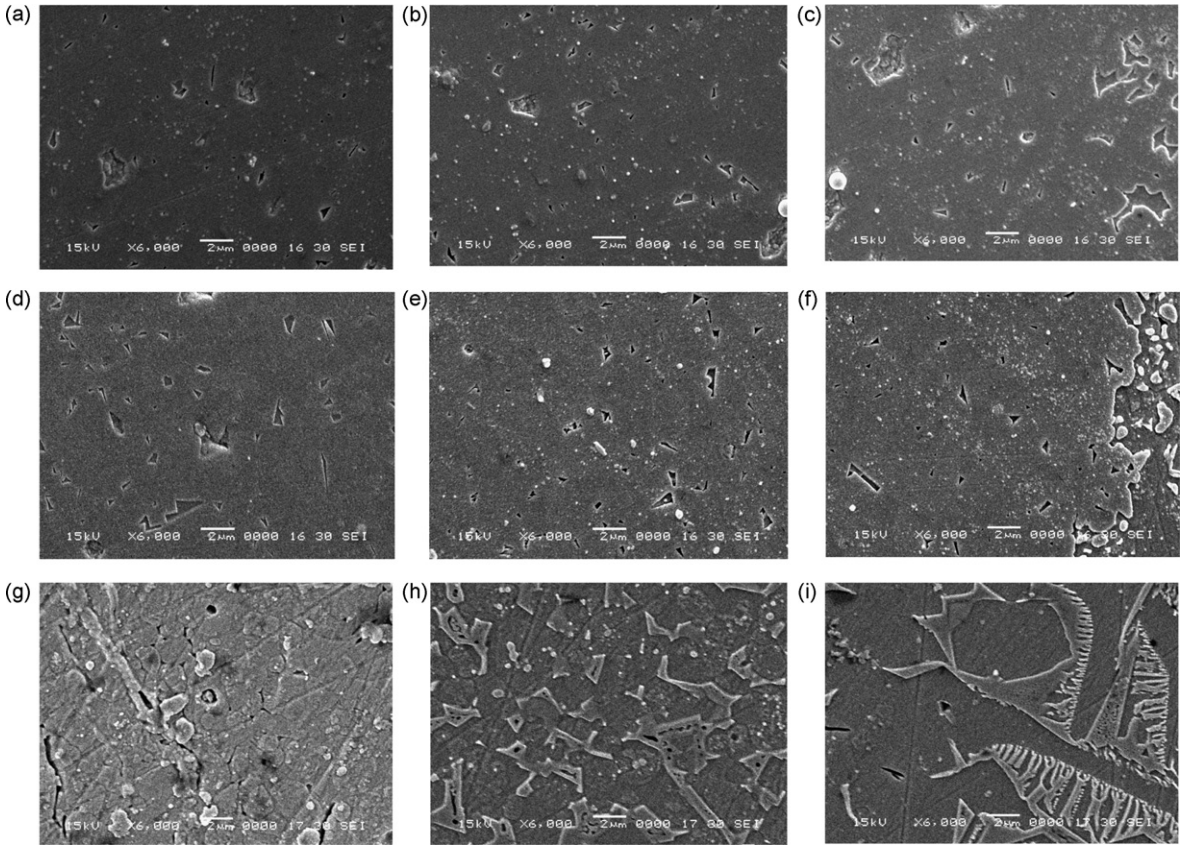

Fig. 8. SEM photomicrograph of three zones of the cordierite cross-section after 10 min ((a) distant extreme of the G2 glass/cordierite interface; (b) middle zone; (c) zone adjacent to G2 glass/cordierite interface); 120 min ((d) distant extreme of the G2 glass/cordierite interface, e: middle zone; (f) zone adjacent to G2 glass/cordierite interface) and 360 min ((g) distant extreme of the G2 glass/cordierite interface; (h) middle zone; (i) zone adjacent to G2 glass/cordierite interface). Bars = 2 μm.

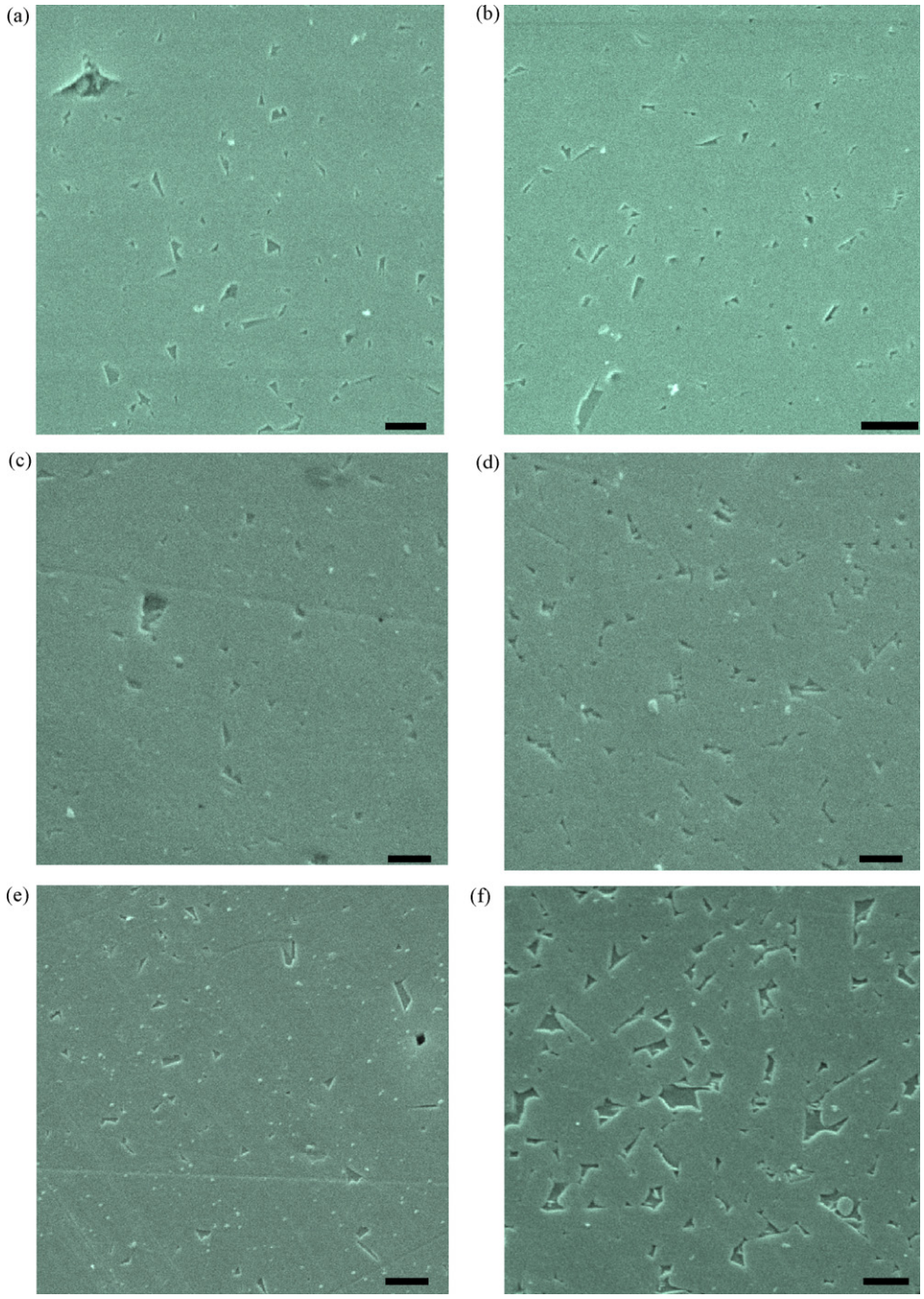

Fig. 9. SEM photomicrograph of three zones of the cordierite cross-section after 10 min ((a) distant extreme of the G1 glass/mullite interface; (b) zone adjacent to G1 glass/mullite interface); 120 min ((c) distant extreme of the G1 glass/mullite interface; (d) zone adjacent to G1 glass/mullite interface) and 360 min ((e) distant extreme of the G1 glass/mullite interface; (f) zone adjacent to G1 glass/mullite interface). Bars = 1 μm.

equilibrium composition is achieved could occur. This reaction could produce the necessary driving force in order to ease the penetration process [18,19,22,23]. Taking this into account, the possible occurrence of the overlapped events of crystallization, penetration, and solution reaction during the penetration tests of this glass into cordierite substrates should be assumed.

Moreover, G1 has the equilibrium liquid composition at 1450 °C, consequently, no change in phase composition occurs in contact with cordierite substrate or, at least, the liquid could dissolve some of the solid and become supersaturated due to the high interfacial free energy and chemical reactivity of the grain boundaries.

SEM photomicrographs of the microstructures resulting along the cross-section of G1 and G2 liquid/mullite interfaces are shown in Figs. 9 and 10, respectively. Significant differences in the penetration features in either glasses on both types of substrates were not appreciated. For both glasses, the penetration increased as the time did, as occurred in cordierite substrates. G1 and G2 glasses were located in triple points and grain–grain interfaces. Moreover, at the longer time,

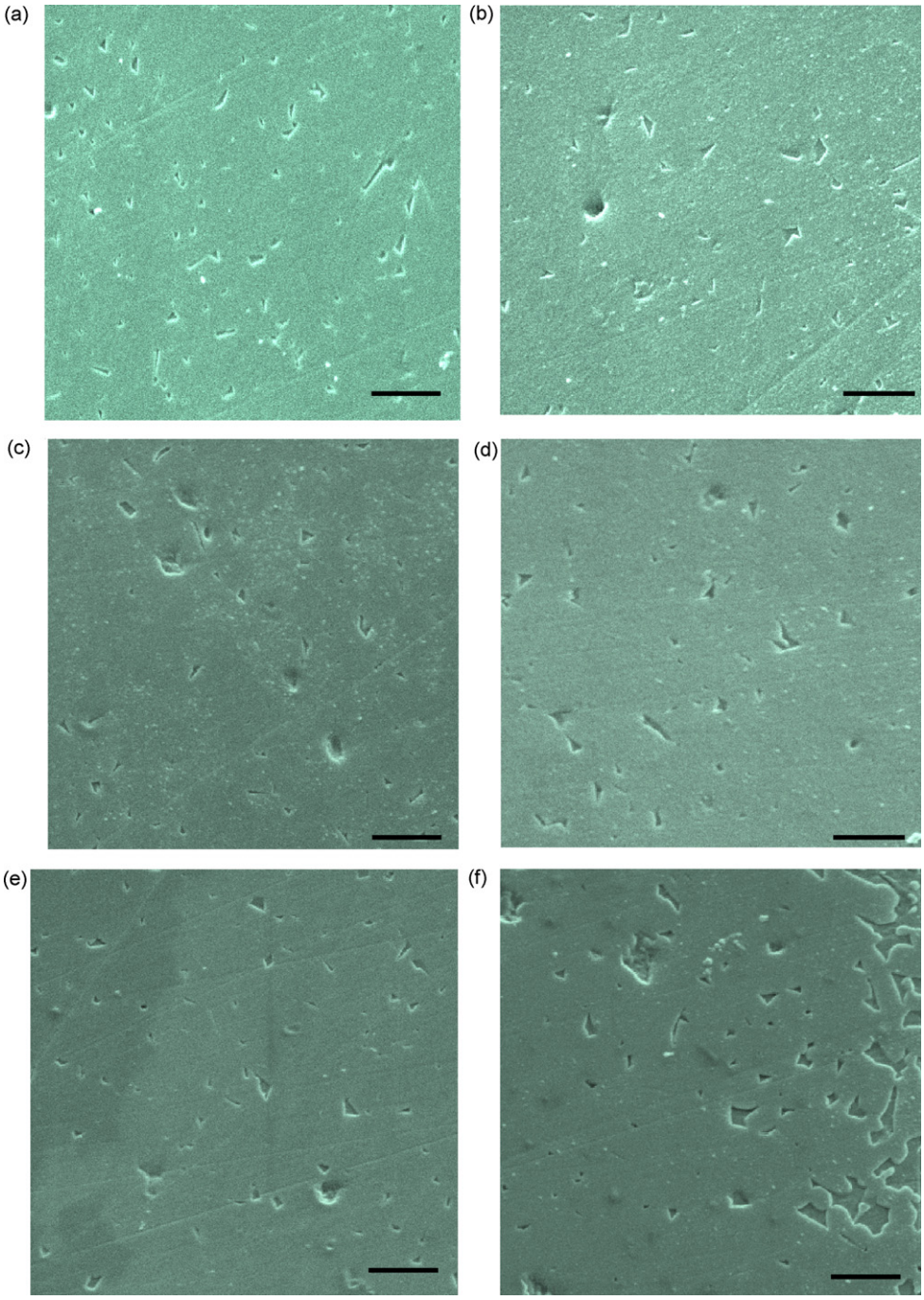

Fig. 10. SEM photomicrograph of three zones of the cordierite cross-section after 10 min ((a) distant extreme of the G2 glass/mullite interface; (b) zone adjacent to G2 glass/mullite interface); 120 min ((c) distant extreme of the G2 glass/mullite interface; (d) zone adjacent to G2 glass/mullite interface) and 360 min ((e) distant extreme of the G2 glass/mullite interface; (f) zone adjacent to G2 glass/mullite interface). Bars = 1 μm.

a significant penetration along two-grain interfaces was appreciated. However, in all the samples, there is no evidence of crystallization as was observed in both glasses on cordierite substrates. Although the temperatures of the tests were the same as those employed with cordierite substrates, the crystallization of G1 and G2 glasses resulted invalid by a kinetic factor. However, the submicronic grains present in the cordierite substrates could have been working as seeds in order to give birth to glass crystallization. This fact is supported by the occurrence of a surface crystallization mechanism in the studied cordierite glasses [13].

4. Conclusions

The non-stoichiometric cordierite glasses studied exhibited better wettability on cordierite than on mullite as-sintered substrates, although, complete wetting did not occur. The wetting of both glasses on both substrates was increased by

increasing the temperature resulting in greater wettability at highest temperatures. The lower contact angle values determined were in the range of those reported by similar systems. However, taking into account the similar surface conditions of both substrates, these values could be overestimated.

Two different types of location of the glasses, three-grain junctions and grain–grain interfaces, were distinguished as features of penetration of the studied glasses into the cordierite and mullite substrates. Both glasses penetrated across mainly open pores of both substrates and the penetration degree increased by increasing time. However, the occurrence or not of crystallization of these glasses and the crystallization rate depended on the substrate type. For cordierite substrates, G1 glass shown fast crystallization and G2 a similar crystallization at the longer time studied. In this case, the submicronic grains present in the cordierite substrates could have been working as seeds in order to give birth to glass crystallization. In addition, for G2 glass, it could be considered the evolution of the glass present into cordierite substrate until equilibrium composition at 1400 °C from the consequent solution reaction in the solid–liquid interfaces. Consequently, the occurrence of the overlapped events of crystallization, penetration, and solution reaction during the penetration tests of this glass into cordierite substrates could be possible. In opposition to both glasses behaviour into cordierite substrates, for mullite substrates, the G1 and G2 glasses did not crystallize during penetration test, the fact that was attributed to a kinetic factor.

Acknowledgements

The authors are grateful to Dras. Alicia Durán and Socorro Benito Bernabé (Institute of Ceramics and Glass, Madrid, Spain) for the realization of the viscosity and contact angle measurements.

References

[1] R.R. Tummala, Ceramic and glass–ceramic packaging in the 1990s, J. Am. Ceram. Soc. 74 (1991) 895–908.
[2] M.A. Subramanian, D.R. Corbin, U. Chowdhry, Better ceramic substrates through zeolites, Bull. Mater. Sci. 16 (6) (1993) 665–678.
[3] K. Niwa, Recent progress in ceramic substrates for microelectronic packaging, in: Ceramic Transactions, Materials in Microelectronic and Optoelectronic Packaging, vol. 33, 1994, pp. 115–124.
[4] J.D. Hodge, Densification and microstructural aspects of mullite–cordierite ceramics, Adv. Ceram. 19 (1986) 117–129.
[5] T. Ebadzadeh, W.E. Lee, Effect of impurities on wetting of mullite by cordierite liquid, J. Mater. Sci. Lett. 18 (1999) 171–172.
[6] R.M. German, Sintering Theory and Practice, John Wiley & Sons, Inc., New York, 1996.
[7] J. Jean, T.K. Gupta, Liquid-phase sintering in the glass–cordierite system, J. Mater. Sci. 27 (1992) 1575–1584.
[8] F. Cambier, A. Leriche, Materials Science and Technology, in: R.W. Cahn, P. Haasen, E.J. Kramer, R.J. Brook (Eds.), Processing of Ceramics Part II, vol. 17B, New York, 1996, pp. 128–129.
[9] M.A. Camerucci, G. Urretavizcaya, A.L. Cavalieri, Sintering of cordierite based materials, Ceram. Int. 29 (2003) 159–168.
[10] M.A. Camerucci, Desarrollo y evaluación de materiales cerámicos de cordierita y cordierita-mullita, Ph.D. Thesis, Universidad Nacional de Mar del Plata, 1999.
[11] R.M. Smart, F.P. Glasser, The subsolidus phase equilibria and melting temperatures of $MgO–Al_2O_3–SiO_2$, Ceram. Int. 7 (3) (1981) 90–97.
[12] M. Nogami, S. Ogawa, K. Nagasaka, Preparation of cordierite glass by the sol–gel process, J. Mater. Sci. (1989) 4339–4342.
[13] N.J. Azín, M.A. Camerucci, A.L. Cavalieri, Crystallisation of non-stoichiometric cordierite glasses, Ceram. Int. 31 (2005) 189–195.
[14] M.D. Glendening, W.E. Lee, Microstructural development on crystallizing hot-pressed pellets of cordierite melt-derived glass containing B_2O_3 and P_2O_5, J. Am. Ceram. Soc. 79 (3) (1996) 705–713.
[15] F.J. Torres, J. Alarcón, Effect of additives on the crystallization of cordierite-based glass–ceramics as glazes for floor tiles, J. Eur. Ceram. Soc. 23 (2003) 817–826.
[16] P. Amista, M. Cesari, A. Montenero, G. Gnappi, L. Lan, Crystallisation behaviour in the system $MgO–Al_2O_3–SiO_2$, J. Non-Cryst. Solids 192/193 (1995) 529–533.
[17] A.L. Cavalieri, P. Pena, S. de Aza, Mullita: naturaleza de la fusión y rango de solución sólida, Bol. Soc. Esp. Ceram. Vidr. 29 (3) (1990) 171–176.
[18] S. Ribeiro, S.P. Taguchi, F.V. Motta, R.M. Balestra, The wettability of SiC ceramics by molten $E_2O_{3(ss)}$/AlN ($E_2O_{3(ss)}$ = solid solution of rare earth oxides), Ceram. Int. 33 (4) (2007) 527–530.
[19] F.V. Motta, R.M. Balestra, S. Ribeiro, S.P. Taguchi, Wetting behaviour of SiC ceramics part I. E_2O_3/Al_2O_3 additive system, Mater. Lett. 58 (2004) 2805–2809.
[20] S.J. Hitchcok, N.T. Carroll, M.G. Nicholas, Some effects of substrate roughness on wettability, J. Mater. Sci. 16 (1981) 714–732.
[21] J. Vila, M.C. Muñoz, C. Valentín, M. Sales, J. Alarcón, Cristalización de cordierita a partir de geles y vidrios estequiométricos. Estudio comparativo, Bol. Soc. Esp. Ceram. Vidrio 38 (1999) 21–28.
[22] P.L. Flaitz, J.A. Pask, Penetration pf polycrystalline alumina by glass at high temperatures, J. Am. Ceram. Soc. 70 (7) (1987) 449–455.
[23] D.A. Weirauch Jr., J.E. Lazaroff, P.D. Ownby, Wetting in an electronic packaging ceramic system: II, wetting of alumina by silicate glass melt under controlled p_{O_2} conditions, J. Am. Ceram. Soc. 78 (11) (1995) 2923–2928.